

Analytical Theory of Susceptibility Induced NMR Signal Dephasing in a Cerebrovascular Network

V. G. Kiselev^{1,2,*} and S. Posse¹

¹*Institute of Medicine, Research Center Jülich GmbH, D-52425 Jülich, Germany*

²*Institute of Physics, Skaryna Avenue 70, 220602 Minsk, Byelorussia*

(Received 12 March 1998)

A deterministic analytical model which describes the time course of NMR signal relaxation in media where the magnetic field is perturbed by stochastic low-density inclusions having one-dimensional extent is developed. Both static and diffusion dephasing mechanisms are included. The model is applied to a simulation of a living tissue where the inclusions are identified with blood microvessels. This application is a ground for quantitation of signal changes during brain activation measured by functional magnetic resonance imaging. The results are consistent with previous Monte Carlo simulations. [S0031-9007(98)07980-0]

PACS numbers: 87.59.Pw, 76.60.Jx, 76.60.Pc, 87.40.+w

The theory of NMR signal dephasing distinguishes between microscopic molecular relaxation mechanisms, and dephasing due to the susceptibility induced magnetic field inhomogeneities at mesoscopic scales. While the theory of molecular relaxation mechanisms is well established, the mesoscopic effects have recently attracted particular interest due to rapid development of functional magnetic resonance imaging (fMRI) of human brain. In this Letter, we find the complete NMR signal relaxation curve in media where the magnetic field is perturbed by stochastic low-density inclusions having one-dimensional extent. Although our theory can be applied to related problems in material science, here we concentrate here on an application to fMRI for which case the inclusions are identified with small blood vessels.

Functional fMRI is a powerful noninvasive tool which employs susceptibility sensitive NMR imaging techniques to study functional brain activations *in vivo* with a typical spatial resolution of a few millimeters and with a temporal resolution of a few seconds. The signal changes in fMRI are due to blood magnetic susceptibility variations associated with brain activations. A local neuronal excitation results in a regional increase in the oxygen consumption, followed by a disproportionally large increase in cerebral blood flow. This vascular overcompensation increases the net oxygenation of venous blood, which is paramagnetic in its deoxygenated state while other tissue components as well as oxygenated blood are diamagnetic. The increase in blood oxygenation reduces the magnetic field inhomogeneity from the vascular network which, in turn, reduces the susceptibility induced signal dephasing in surrounding tissue (brain parenchyma). Thus, the signal intensity in the activated region increases. This blood oxygenation level dependent contrast mechanism is called BOLD effect [1]. In practice, one repeats measurement with and without the physiological stimulus (e.g., light switched on and off) and searches for temporal correlations between the stimulus and the brightness of image pixels [2].

The first goal of a theory is to describe the complete signal relaxation curve as a function of physical characteristics of blood and tissues. The latter are subject to physiological changes which are slow as compared with the signal relaxation (a few seconds v.s. ≈ 70 ms at 1.5 T). Such a theory is highly desirable for quantitating fMRI in terms of well-defined physiological parameters (e.g., the changes in blood oxygenation level and flow) which is currently not feasible. This theory is of particular importance, since with recent technical advances such as [3,4], one can measure the complete signal relaxation curve for each pixel.

The pioneering works in building a signal relaxation model in line with the above requirements were a Monte Carlo simulation [5] and an analytical model based on the Anderson mean field theory [6]. The most comprehensive existing model is based on a Monte Carlo simulation of the proton random walk in a stochastic vascular network [7]. However, Monte Carlo simulations are computationally intense and do not allow study of the relative contributions of various underlying dephasing mechanisms. An analytical approach to the stochastic microvasculature was developed in [8]. However, that paper did not consider the effect of diffusion which is important for the signal dephasing around capillaries and venules.

Here we develop an analytical treatment of the signal dephasing based on a tissue model similar to those used in papers [7,8]. In common with [7], we account for the diffusion dephasing. For this purpose, we generalize the basic equation of [8] which derives the signal time course from the dephasing in the vicinity of a single vessel. The explicit calculations are performed in two limiting cases called the static dephasing regime (SDR, section II-A) and the diffusion narrowing regime (DNR, section II-B). The parameters of our model are as follows: B_0 , the main magnetic field; χ , the magnetic susceptibility of blood relative to that of parenchyma; D , the apparent water diffusion coefficient; $\zeta(R)$, the differential volume fraction of blood vessels with radius R ; T_2 , the transverse relaxation

time which is due to the microscopic spin-spin interaction and is not affected by physiological changes. There are no adjustable parameters in our model.

(I) *Basic theory.*—Each image voxel (volume element) contains many microvessels. This suggests an averaging over the microvessel distribution which is commonly assumed. We consider only voxels which are macroscopically homogeneous. The signal from such a voxel takes the following form when normalized to its initial value:

$$S(t) = \exp(-i\omega_0 t) \exp\left(-\frac{t}{T_2}\right) s(t). \quad (1)$$

Here $\omega_0 = \gamma B_0$ is the Larmor frequency of spin precession (γ is the gyromagnetic ratio), and $s(t)$ describes the signal dephasing in the magnetic field induced by the microvascular network at the mesoscopic length scale (a few μm and larger). We call $s(t)$ the signal attenuation factor. The task of our theory is to calculate this function.

(A) The tissue model: We consider the brain parenchyma as a homogeneous medium where the water molecules diffuse freely and isotropically, but the diffusion coefficient is reduced as compared to that of pure water. This is a good approximation for cortical brain areas where $D = 0.76 \mu\text{m}^2/\text{ms}$ [9].

The microvascular network consists of interconnecting segments which are nearly straight and much longer than their diameter. This is modeled as a set of statistically independent cylinders with random positions $\vec{\rho}_n$, orientations θ_n , and radii R_n . The distributions of the cylinder position and orientation are uniform. The cylinder radius distribution is characterized by $\zeta(R)$ which is the differential volume fraction of cylinders with radius R . This function is normalized to the total blood volume fraction ζ_0 :

$$\int \zeta(R) dR = \zeta_0. \quad (2)$$

Our approach will be applicable only to small ζ_0 which is the case for the brain tissues where $\zeta_0 = 3\% - 5\%$.

The vessel walls are partly permeable for water molecules. In our calculations, the effect of cylinder boundary permeability is subdominant for relatively large vessels described in the SDR. We thus assume impermeable vessel walls in this regime. For the capillaries described in the DNR, we assume freely permeable vessel walls. In both regimes, the effect of a finite vessel wall permeability is small [7].

Consider a spin packet placed at the origin of a coordinate system $\vec{r} = 0$. The local frequency of spin precession is

$$\Omega = \omega_0 + \sum_{n=1}^N \omega(\vec{\rho}_n; R_n, \theta_n). \quad (3)$$

Here $N \gg 1$ is the number of cylinders and $\omega(\vec{\rho}_n; R_n, \theta_n)$ is the Larmor frequency offset caused by the magnetic field from the n th cylinder:

$$\omega(\vec{\rho}; R, \theta) = \begin{cases} \delta\omega \frac{R^2}{\rho^2} \cos 2\varphi \sin^2 \theta & \text{for } \rho > R, \\ \delta\omega (\cos^2 \theta - \frac{1}{3}) & \text{for } \rho < R, \end{cases} \quad (4)$$

where $\rho = |\vec{\rho}|$ and φ are the radius and the azimuthal angle in the plane orthogonal to the cylinder, θ is the angle between the cylinder and the direction of the main magnetic field, and $\delta\omega = 2\pi\gamma\chi B_0$. The expression for ω inside the vessel is based on the Lorentz sphere construction for an estimate of the magnetic field affecting the atomic nuclei [10]. We do not take into account the additional correction term in ω for $\rho < R$ [10].

The magnetization density η of the spin packet at a space point \vec{r} at time t is the fundamental solution of the Bloch-Torrey equation [11]

$$\begin{aligned} \frac{\partial \eta(\vec{r}, t)}{\partial t} &= D\Delta \eta(\vec{r}, t) - i\Omega(\vec{r})\eta(\vec{r}, t), \\ \eta(\vec{r}, 0) &= \delta(\vec{r}). \end{aligned} \quad (5)$$

The total magnetization of the spin packet is

$$\Psi(t) = \int \eta(\vec{r}, t) d\vec{r}. \quad (6)$$

For practical calculations, the path integral representation for η can be useful.

(B) Averaging over the vessel distribution: The observed signal attenuation factor takes the form

$$s(t) = \int \Psi(t) \prod_{n=1}^N d\Gamma_n, \quad (7)$$

where $d\Gamma$ stands for the integrations necessary for averaging over the position and orientation of a given cylinder. The small blood volume fraction justifies a factorization

$$\Psi(t) = \prod_n \psi(t, \rho_n, \theta_n), \quad (8)$$

where ψ is the factor contributed by one cylinder. The correction terms to this formula are of the order of ζ_0^2 in the exponent. Note that $s(t)$ given by (7) is equivalent to the statistical sum of cylinders in a potential induced by $\Psi(t)$. From this point of view, the statistical independence of cylinders and Eq. (8) are equivalent to neglecting the contact interaction between cylinders and their indirect interaction induced by the spin packet. Both approximations are valid when $\zeta_0 \ll 1$. They result in the following form of the signal attenuation factor:

$$\begin{aligned} s(t) &= \prod_n \left[1 - \int [1 - \psi(t, \rho, \theta)] d\Gamma \right] \\ &= \exp \left[- \int \zeta(R) f dR \right], \end{aligned} \quad (9)$$

where

$$f = \frac{1}{\pi R^2} \int [1 - \psi(t, \rho, \theta)] d\Gamma \quad (10)$$

is a function of two dimensionless parameters $\tau = \delta\omega t$ and $\lambda = D/R^2 \delta\omega$. The value $\pi R^2 f$ can be thought of as an effective area in the plane orthogonal to the vessel where the dephasing takes place.

Equations (9) and (10) form the general framework for calculation of the relaxation rate. In the rest of this paper, we find the explicit form of the f function for the cases of SDR and DNR.

(II) *Explicit expressions and results.*—The starting point of our calculations is to solve equation (5). This can be done in the two following approximations which we express in terms of the diffusion length $l_D = \sqrt{Dt}$ and diffusion time $t_D = R^2/D$: (i) The SDR when $l_D^2/R^2 = \lambda\tau \ll 1$. In the SDR, the spin packets evolve in a nearly uniform field. This is always valid for short measurement times and for sufficiently large vessels; (ii) the DNR when $t_D\delta\omega = 1/\lambda \ll 1$. In the DNR, the diffusion is so fast that the spins are resident in the vicinity of a vessel for a relatively short time. The applicability of this approximation does not depend on t . Thus the validity regions of DNR and SDR overlap for $t \ll 1/\delta\omega$ (where they give the same predictions). For larger times, the two approximations deliver complementary information

$$f(\tau; \lambda) = \int_0^\pi \frac{\sin\theta d\theta}{2} \left\{ \int_0^1 \left[1 - \exp\left(-\frac{4}{3}\lambda\tau^3 u^3 \sin^4\theta\right) J_0(\tau u \sin^2\theta) \right] \frac{du}{u^2} - \exp\left[-i\tau\left(\cos^2\theta - \frac{1}{3}\right)\right] \right\} + 1, \quad (11)$$

$$f_E\left(\tau; \lambda, \frac{\tau_E}{\tau}\right) = \int_0^\pi \frac{\sin\theta d\theta}{2} \int_0^1 \left\{ 1 - \exp\left[-\frac{4}{3}\lambda\tau^3 F\left(\frac{\tau_E}{\tau}\right) u^3 \sin^4\theta\right] J_0(|\tau_E - \tau|u \sin^2\theta) \right\} \frac{du}{u^2}, \quad (12)$$

where $u = R^2/\rho^2$, $\tau_E = \delta\omega T_E$, and $F(z) = 1 - 3z^2/2 + 3z^3/4$. The first and the second terms in the integral over θ in (11) are the contributions of the protons from outside and inside the vessels, respectively. The functions (11) and (12) are plotted in Fig. 1(a). For many practical applications, it is sufficient to use the long-time asymptotic forms of these functions for $\tau \gg 1$ which are

$$f(\tau; \lambda) \approx \left(\frac{2}{3} + C_1\lambda\right)\tau + \sqrt{\frac{\pi}{4\tau}} \exp\left(-i\frac{\tau}{3} - i\frac{\pi}{4}\right), \quad (13)$$

$$f_E(\tau_E; \lambda, 1) \approx C_2\lambda^{1/3}\tau_E - 1, \quad (14)$$

where $C_1 = 1.659$, $C_2 = 0.694$ (the term $2\tau/3$ was first found in [8]).

(B) *Diffusion narrowing regime:* In the DNR, the magnetic field of the blood vessels has a relatively small effect on the spin precession phases and Eq. (5) can be solved perturbatively in ω . We expand η in powers of ω : $\eta = \eta^{(0)} + \eta^{(1)} + \eta^{(2)} + \dots$. Other values are expanded and labeled accordingly. The zeroth order term $\eta^{(0)}$ is the conventional Green function for the free diffusion. In terms of the Fourier components $\tilde{\eta}(\nu, \mathbf{k})$ and $\tilde{\omega}(\mathbf{k})$ (ν and \mathbf{k} are the frequency and the wave vector in the plane orthogonal to the cylinder, respectively), $\tilde{\eta}^{(0)}(\nu, \mathbf{k}) = 1/(D\mathbf{k}^2 - i\nu)$, $\psi = 1$, and thus $f^{(0)} = 0$. In the next 2 orders of perturbation theory, the f function takes the following form:

about the signal dephasing by small and large vessels, respectively. Below, we consider both of them separately.

The signal decay measured after an excitation is commonly referred to as the free induction decay (FID). Also commonly used is the spin-echo (SE) experiment which employs a refocusing radiofrequency pulse at time $T_E/2$. This pulse reverses the spin precession phases, thus causing the spin rephasing and creation of the so-called spin echo at the echo time T_E . We shall concentrate on the treatment of the FID and present only the results for the SE experiment for which the corresponding f function will be referred to as f_E .

(A) *Static dephasing regime:* In the SDR, the magnetic field across the size of the spin packet can be approximated by the first two terms of the Taylor expansion: $\omega(\vec{r}) \approx \omega(0) + \vec{r}\nabla\omega(0)$. This reduces the problem to diffusion in a constant-gradient magnetic field which is exactly solvable. The detailed calculations will be published in [12]. The results take the following form:

$$f^{(1)} = \frac{it}{\pi R^2} \int \frac{\sin\theta d\theta}{2} \tilde{\omega}(0), \quad (15)$$

$$f^{(2)} = \frac{1}{\pi R^2} \int \frac{\sin\theta d\theta}{2} \int \frac{d^2\mathbf{k}}{(2\pi)^2} g_2(t, D\mathbf{k}^2) \tilde{\omega}(\mathbf{k}) \tilde{\omega}(-\mathbf{k}), \quad (16)$$

where $g_2(t, z) = [\exp(-tz) - 1 + tz]/z^2$.

Finally, we find $\tilde{\omega}$ using (4). The first-order function (15) vanishes due to the term $\cos^2\theta - 1/3$ in (4). The f functions are dominated by the second order terms which take the form

$$f(\tau, \lambda) = \frac{32}{45\lambda^2} \int_0^\infty g_2(\lambda\tau, z) \frac{J_1^2(z)}{z} dz, \quad (17)$$

$$f_E(\tau, \lambda) = \frac{32}{45\lambda^2} \int_0^\infty [g_2(a_1, z) + g_2(a_2, z) - g_1(a_1, z)g_1(a_2, z)] \frac{J_1^2(z)}{z} dz, \quad (18)$$

where $a_1 = \lambda\tau_E/2$, $a_2 = \lambda\tau - \tau_E/2$, and $g_1(t, z) = [\exp(-tz) - 1]/z$ [Fig. 1(b)]. Note that the combination $\lambda^2 f$ depends on the only argument $\lambda\tau = t/t_D$.

For short measurement times, f takes its asymptotic form $f = 8\tau^2/15 + 4\lambda\tau^3/15$ which coincides with that for the SDR as expected. For large times $\lambda\tau \gg 1$,

$$f(\tau, \lambda) \approx \frac{4}{45\lambda^2} \left[\frac{t}{t_D} \left(\ln \frac{t}{t_D} + C_3 \right) + \frac{1}{4} \ln \frac{t}{t_D} + C_4 \right], \quad (19)$$

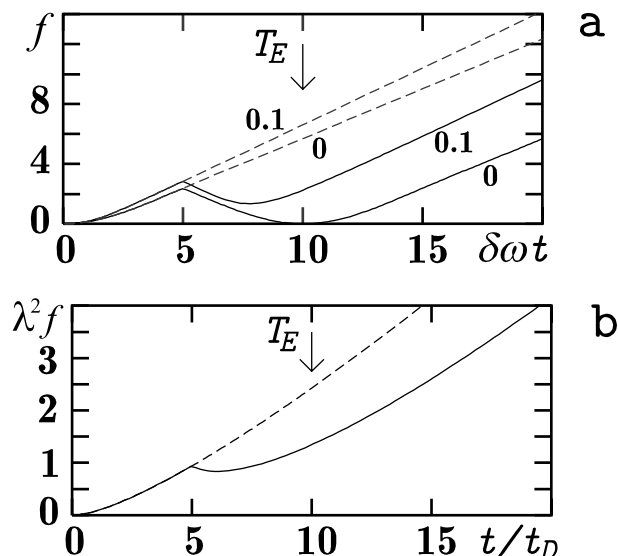


FIG. 1. f function (10) for the FID (dashed lines) and the SE experiments (solid lines) with a refocusing pulse applied at $t/t_D = 5$. (a) f in SDR vs $\delta\omega t$ for the indicated values of λ . (b) $\lambda^2 f$ in DNR vs t/t_D .

where $C_3 = 0.309$ and $C_4 = 0.619$. The function f_E measured at large $t = T_E$ takes the same form with a prefactor of 8 instead of 4, and t/t_D and C_3 replaced with $t/2t_D$ and $C_3^E = -0.384$, respectively.

A comparison of our results with the predictions of the Monte Carlo simulation [7] (Fig. 2) shows a very good agreement for both the DNR and SDR. The simplest way to describe the crossover region is to write interpolation formulas between the corresponding long-time asymptotic forms. This can be sufficient for the practical applications because the time scale $\tau \sim 1$ is rather short (for the typical values $B_0 = 1.5$ T and $\chi = 10^{-7}$ it is 4 ms while the measurement time is usually $t = 40$ – 100 ms).

An interesting finding of our theory is the difference in the shape of the relaxation curves for small and large vessels [Fig. 1, Eqs. (13), (14), and (19)] which may help to experimentally distinguish their relaxation contributions.

It follows from comparison of Eqs. (13) and (14) (see also Fig. 1a) that the conventionally used formula for the transverse relaxation rates of FID: $1/T_2^* = 1/T_2 + 1/T_2'$ fails where T_2 is separately measurable in the SE experiment and $1/T_2'$ is the contributions of the reversible static dephasing. This is a result of the statistical dependence of diffusion and static dephasing mechanisms, because both of them are due to the same blood vessels. A more detailed discussion of the SDR results will be presented in [12].

The obtained results can be applied to NMR signal relaxation in media other than living tissues where the magnetic field is perturbed by stochastic low-density inclusions having one-dimensional extent. The isotropic inclusion distribution $(\sin \theta)/2$ can be easily modified in our final expressions to account for possible anisotropy.

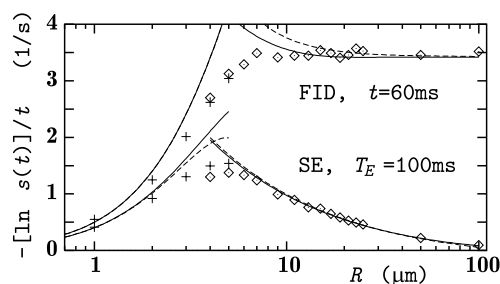


FIG. 2. The signal attenuation factor as predicted by the presented theory (solid lines) in comparison with the corresponding results of the Monte Carlo simulation [7] for monosized vessels with radius R for $B = 1.5$ T, $D = 1 \mu\text{m}^2/\text{ms}$, $\chi = 1 \times 10^{-7}$, $\zeta(R) = 2\%$. The approximation of DNR (small R) is compared with the data for permeable vessels (crosses), the SDR results (large R) are compared with the data for impermeable vessels (diamonds). The dashed lines show the corresponding asymptotic formulas (13), (14), and (19) and the modification for the SE signal described in the text thereafter (the dashed and solid lines are indistinguishable for the FID in the DNR).

Applications to *in vivo* fMRI experiments require one to feed the model with the real vascular size distribution $\zeta(R)$, D , and χ . This work will be reported elsewhere.

We are grateful to A. Berezhkovskii, P. Grassberger, K. Kehr, H.M. Krenzlin, J.N. Shah, J.G. Taylor, and S. Wiese for useful discussions and to the European Union for supporting this work through BioMed Grant No. PL 950870.

*Corresponding author.

Email address: v.kiselev@fz-juelich.de

- [1] S. Ogawa *et al.*, Proc. Natl. Acad. Sci. U.S.A. **87**, 9868 (1990).
- [2] We do not consider here the imaging technique [for that see, e.g., P. Mansfield and P.G. Morris, *NMR Imaging in Biomedicine* (Academic Press, New York, 1982)]. Actually, we discuss the signal dephasing in one volume element (voxel) already selected from the image.
- [3] S. Posse *et al.*, in *Proceedings of the International Societies for Magnetic Resonance in Medicine, 1997* (Society of Magnetic Resonance, Berkeley, CA, 1997), p. 376.
- [4] O. Speck and J. Hennig, Magn. Reson. Med. **40**, 243 (1998).
- [5] S. Ogawa *et al.*, Biophys. J. **64**, 803 (1993).
- [6] R.P. Kennan, J. Zhong, and J.C. Gore, Magn. Reson. Med. **31**, 9 (1994).
- [7] J.L. Boxerman *et al.*, Magn. Reson. Med. **34**, 555 (1995).
- [8] D.A. Yablonskiy and E.M. Haacke, Magn. Reson. Med. **32**, 749 (1994).
- [9] D. Le Bihan, R. Turner, and N. Patronas, in *Diffusion and Perfusion. Magnetic Resonance Imaging: Applications to Functional MRI*, edited by D. Le Behan (Raven Press, New York, 1995), p. 134.
- [10] W.C. Dickinson, Phys. Rev. **81**, 717 (1951).
- [11] H.C. Torrey, Phys. Rev. **104**, 563 (1956).
- [12] V.G. Kiselev and S. Posse, Magn. Reson. Med. (to be published).